Analysis of high-voltage low-current DC/DC converters for electrohydrodynamic pumps

Independent project work

Sigge Axelsson, Jonas Gartner, Axel Stafström

Master's programme in electrical engineering
Examensarbete 15 hp
19th June 2023

Abstract

Moving parts cause vibrations and tend to wear out. In applications where maintenance is complicated, solutions without moving parts are therefore advantageous. Electrohydrodynamic pumps are such a solution. Instead of mechanical propulsion, they use strong electric fields to induce movement in a dielectric cooling liquid. These pumps require very little power, but to generate sufficiently strong electric fields, they need to be fed with very high voltage.

This project explored various methods for designing DC/DC-converters which fulfil the demands of an electrohydrodynamic pump. This was done by altering and combining existing topologies that were deemed to be relevant. The main method for testing and evaluation was by simulating in LTspice. The project also briefly investigated methods of overcurrent protection. This was relevant because gas bubbles in the cooling fluid can cause electric arcs which damage the pumps.

Three converter topologies were chosen for further evaluation. First, a conventional resonant Royer-based converter that has previously been used by APR Technologies which was altered by the inclusion of a feedback loop. Second, a high-frequency resonant Royer-based converter with a planar air-core transformer. Third, a transformerless converter with a switched boost converter IC. All circuits included a Cockroft-Walton voltage multiplier bridge.

The two resonant Royer-based converters fulfilled all requirements except the one on efficiency, while the transformerless converter fulfilled all requirements except the one on cost, set by APR. The more expensive transformerless converter had a significantly higher efficiency and a wider range of acceptable input voltages.

Furthermore three general conclusions were drawn. The first was that planar air-core transformers are not beneficial compared to conventional transformers in these type of applications. The second was that a discrete voltage regulator controlled by feedback from the output is more effective than using a voltage regulator without feedback, as it also eliminates temperature and load variations. The third conclusion was that to protect the circuits from overcurrent, a large series resistor is needed, which causes significantly lowered efficiency.

I

Contents

1 Introduction

1.1 Background

Engineers often aim to avoid moving parts in their designs as these tend wear out and cause vibrations. Such considerations are especially important in applications where maintenance is complicated, such as in space or in telecommunication towers [1]. Examples of components that are often subject to long term failure are cooling fans and pumps. In an effort to solve this problem, APR Technologies have developed electro-hydrodynamic cooling systems that utilise strong electric fields to generate liquid flow without the use of moving parts [1].

These pumps require very little power, but to generate sufficiently strong electric fields, they need to be fed with very high voltage. This project investigated various types of electronic power converters that can fulfil this task while being light, cheap and reliable.

1.2 Purpose

The aim of this project is to explore various methods for designing DC/DC converters that are suitable for high voltage low current electrohydrodynamic applications. There is little research on these types of power converters, since the application is very specialised. The investigation will be conducted using established topologies and will primarily consist of LTspice simulations. The converters will be evaluated mainly based on output voltage, efficiency, power, size, weight, cost and reliability. The investigation will be restricted to converters that meet the requirements stated by APR.

1. Input voltage: 12–48 V

2. Output voltage: 1000–3000 V

3. Output power: ≈1.5 W

4. Efficiency: >75 %

5. Drift temperature: -40–60 °C

6. Price: <9 €

7. Size: <10 ∗ 3 ∗ 3 cm

8. Weight: <200 g

Furthermore, a maximum output current of 2 mA in case of an arc was desired, but not required.

2 Theory

2.1 LTspice

LTspice is a SPICE (Simulation Program with Integrated Circuit Emphasis) software developed by the semiconductor manufacturer Linear Technology and is a free and widely-used software tool for simulating electronic circuits. LTspice allows the user to create graphical circuit schematics and also offers the possibility to provide simulation results in graphical form. Many electrical component manufacturers provide models that can be imported to LTspice, making this a very powerful tool for simulating the design of electronic circuits before they are built.

2.2 Gallium nitride transistors

Gallium nitride (GaN) is a semiconducting material which has recently become more popular in transistors [2]. Transistors made with this material have several advantages over regular silicon transistors, such as: higher breakdown voltage, quicker switching and lower on resistance, all with the same or smaller size package [3]. A complication is that extra care is required when designing the driving circuitry, so as to not risk the transistor turning on inadvertently, due to the low charge required to raise the gate voltage making the transistor sensitive [4].

2.3 Resonant Royer oscillator

The resonant Royer oscillator (hereafter simply called the Royer oscillator) is a circuit consisting of two transistors who have their collectors connected to a centre-tapped transformer. The circuit is self oscillating, causing it to induce a sine-like voltage in the secondary winding of the transformer. One of the main benefits of Royer oscillators is that they produce a voltage that is relatively noise free and has low harmonic content [5]. One specific variant of the Royer oscillator can be observed in figure 1. Another variant is presented in chapter 4.4.2 and can be observed in figure 10.
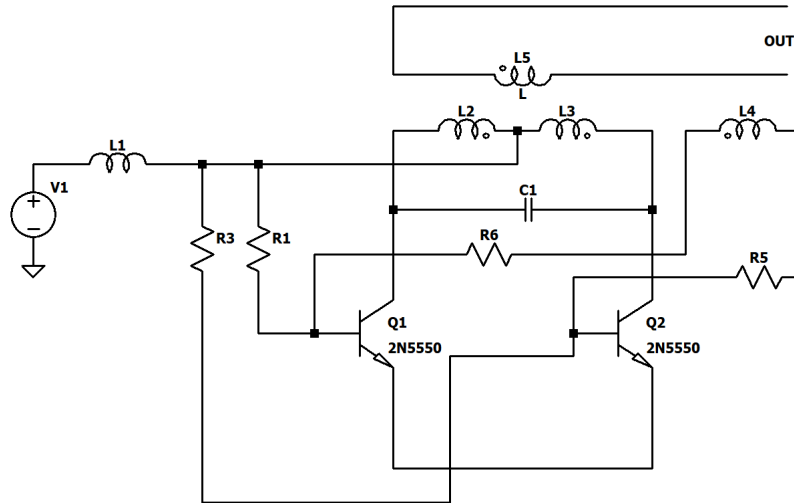
Figure 1: Royer oscillator

The theory of operation for this circuit can be seen as follows. When Q1 and Q2 conduct current, L2 and L3 will induce a magnetic field in the transformer, which then induces a voltage of opposite polarity in L4, lowering the base voltage of Q1 and Q2 until they start conducting in the opposite direction. The rate of oscillation can be adjusted by changing the value of C1. Note that the transistors always conduct in different directions.

2.4   Voltage multiplier

Voltage multipliers are a group of circuits with the ability to generate high DC voltages from an AC or pulsating voltage source, with the benefits of being simple, efficient and with a low cost [6]. The voltage multiplier can be divided in to two categories, voltage multiplier cells (VMC) and voltage multiplier rectifiers (VMR). VMC and VMR have an overlap of included topologies, with the main difference being in the application.

The voltage multiplier cell is a topology often applied inside the circuit of a step-up or step-down converter [6], commonly placed next to the converters primary switch. The purpose of a VMC is to amplify the conversion ratio of step-up or step-down converter compared to what would be achieved with the same duty-cycle in a standard configuration [7]. A VMC consists of diodes, capacitors and not uncommonly an inductor.

A voltage multiplier rectifier is often placed at the output of a circuit generating an AC of pulsating voltage [6], being able to both rectify and multiply the voltage. VMR circuits consist only of diodes and capacitors, often in a ladder topology as seen in figure 2. The main benefits of a VMR is its ability to rectify AC voltages and to easily be cascaded to increase voltage gain. A VMR is commonly seen to increase voltage up to 15 times, and in some cases even 30 times the peak supply voltage. The drawback of the circuit is its susceptibility to ripple and voltage drop during large loads, due to the large

output impedance during many cascaded stages [8]. This makes the VMR best suitable for low current applications [6].

The two most common voltage multiplier rectifier topologies are the Cockroft-Walton voltage multiplier (CWVM) and the Dickson voltage multiplier (DVM). Cockroft-Walton and Dickson voltage multipliers are used to generate high DC voltages and are commonly found in applications like X-ray machines, particle accelerators, photocopiers and integrated circuits, as well as LCD and LED drivers.

Another category commonly found in the literature is the charge pump or switched capacitor converter. The charge pump is a circuit witch uses switches and capacitors that steps-up a lower DC to voltage to a much higher output DC voltage [9] [6]. The charge pump and switched topologies also overlap the previously named voltage multiplier categories with the Cockroft-Walton and Dickson voltage multiplier being categorised as both a charge pump and a voltage multiplier rectifier [10] [6].

This paper will only focus on the voltage multiplier rectifier category of voltage multipliers with a special focus on the Cockroft-Walton voltage multiplier topology.

2.4.1 Crockroft-Walton voltage multiplier

The Crockroft-Walton voltage multiplier (CWVM), which is also known as Greinacher voltage multiplier is a common and established voltage multiplier rectifier topology used for generating high DC voltages from a smaller AC input voltage. The topology is often used in combination with a transformer to rectify and further increase voltage gain [6] or applications where transformers a deemed to bulky of a solution while still needing high voltage gains [11]. Note that the Cockroft-Walton voltage multiplier may be also be referred to as a bridge or simply voltage multiplier.
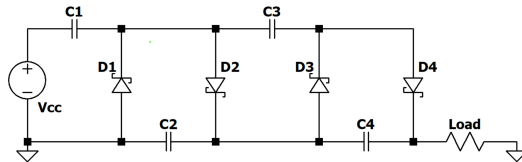
Figure 2: A two-stage half-wave Crockroft-Walton voltage multiplier

A Cockroft-Walton bridge commonly consists of several cascaded stages. See figure 2. Each stage is made up of two capacitors and two diodes. In figure 2, parts C1, C2, D1 and D2 make up the first stage and C3, C4, D3 and D4 make up the voltage multiplier's second stage.

A simplified explanation of the CWVM operation is found below in step a-c, using symbol names found in figure 2. The explanation makes the following assumptions: The CWVM is fed with a symmetrical AC voltage with a peak voltage $\hat{V}_{in}$, the diodes are assumed ideal and the capacitors are fully charged.

a) During the the negative half-cycle, current flows through the forward-biased diode D_1 and charges capacitor C_1 to $\hat{V}_{in}$.

b) During the positive half-cycle, D_1 is revere-biased and conducts no current. C_1 is still charged to $\hat{V}_{in}$ which offsets the AC input voltage to $2\hat{V}_{in}$ over diode D_1. D_2 and C_2 then acts as a rectifier giving out a $2\hat{V}_{in}$ DC voltage.

c) The process then repeats, with the next stage receiving an AC voltage of $\hat{V}_{in}$ while being offset by $2\hat{V}_{in}$ from the previous stage's rectifier.

The voltage multiplication of a Cockroft-Walton multiplier with N stages can be calculated with the peak-to-peak input voltage using equation 1 [8].

$$V_{out} = NV_{in(p-p)} \tag{1}$$

The primary drawback of the Cockroft-Walton voltage multiplier is the voltage drop during large loads [12]. The voltage drop can be qualitatively modelled by equation 2 and is dependent on the voltage multiplier's capacitors C, the switching frequency f, the output current I_o being drawn from the circuit and a constant k which is dependent on the number of stages in the voltage multiplier [12]. By using a high switching frequency and large capacitors, the voltage drop can be minimised. The switching frequency, which is a common way of minimising the voltage drop, is often limited by switching capabilities and by electromagnetic interference appearing when high switching frequencies are used. The size of the capacitors is largely limited by the size of the board, component cost and safety standards to avoid chock hazards.

$$V_{drop} = k\frac{I_o}{C \cdot f} \tag{2}$$

If the same value for all the capacitors are used in the CWVM, the following equation can be used to calculate the output voltage with consideration to voltage drop [13].

$$V_{out} = NV_{p-p} - \frac{I_o}{fC}\frac{4N^3 + 3N^2 + 2N}{6} \tag{3}$$

The capacitors in the bridge are commonly chosen to be of the same capacitance. However, they do not affect the output voltage in the same way or the same amount [10]. Thus, a more optimal design, in terms of voltage ripple, voltage drop and total capacitance, can be created by choosing the capacitors carefully. In [10], the following scheme is concluded to be optimal.

$$C_{2i} = C_{2i-1} = (N + 1 - i)C \tag{4}$$

Where N is the total number of steps, i is the index of a certain step and C is the base capacitance, which is calculated from the frequency, number of steps and the load.

2.4.2 Series-connected positive-negative voltage multiplier

The voltage drop and ripple of a Cocroft-Walton voltage multiplier can be significantly decreased by using a topology called series-connected positive-negative voltage multiplier (SPNVM) [14], see figure 3.

The SPNVM topology consists of two conventional Cockroft-Walton voltage multipliers connected in parallel. One CWVM connected to generate a positive voltage and one connected to generate a negative voltage. The load is then connected between the positive and the negative outputs of the voltage multipliers.

The SPNVM surpasses the performance of a single conventional CWVM with equivalent voltage in terms of ripple, voltage drop and capacitor charging characteristics while using the same components. Approximately 22 % lower voltage drop and 85 % lower voltage ripple factor is reported in [14] compared to a standard CWVM with the same amount of components. Note that the comparison is made without a smoothing capacitor on the output for the standard CWVM.

This makes it possible to use fewer stages and to not include a smoothing capacitor on the output, which in a conventional CWVM would experience a large voltage stress (the entire output voltage).

2.5 LT8331

The LT8331 [15], seen in figure 12, is a current feed DC/DC step-up converter with the ability to generate a high switching voltage (up to 140 V), while being powered from a wide range of input voltages (4.5 V–100 V). It has features such as programmable switching frequencies of up to 500 kHz, programmable output voltage from a negative feedback pin as well as well as being configurable to operate as a wide range of step-up and step-down converters.

The output voltage of the LT8331 is controlled by the negative feedback pin named FBX. The LT8331 feedback functions by regulating the switching frequency and voltage
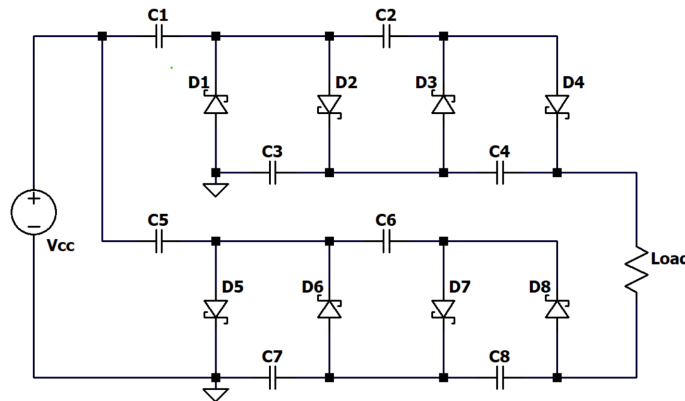

Figure 3: Series-connected positive-negative voltage multiplier

so that 1.6 V is received at the feedback pin. The feedback is connected to a voltage divider configured with equation 5.

$$R_1 = R_2(\frac{V_{OUT}}{1.6} - 1) \tag{5}$$

The LT8331 operates with a switching frequency in the range of 100 kHz to 500 kHz which is controlled by a single resistor connected to the RT-pin. The value of the resistor is chosen with equation 6.

$$R_T = \frac{32.85}{f_{SW}} - 9.5 \tag{6}$$

Other noteworthy features of the LT8331 is soft-start, under-voltage protection and mode-selection. (a) The soft-start function regulates the inductor current and can be programmed by changing the capacitor size connected to the SS-pin. (b) The under-voltage protection shuts off the circuit if a too low input voltage is received and is programmed by a voltage divider connected to the EN/UVLO-pin. (c) With the Sync/mode pin, three different modes of operation can be selected to optimise the circuit's performance.

2.6 Planar PCB-integrated transformers

Planar transformers are a type of transformer where the primary and the secondary side are made of planar inductors, i.e. coils where all turns are in the same plane. They can, for instance, be integrated in a PCB by tracing two coils on top of each other in different layers. This design gives planar transformers several advantages over conventional transformers, with the main one being that they are easy and cheap to mass produce with high repeatability [16]. Another benefit is that the thin and wide copper traces in PCBs cause lower losses due to skin effect compared to conventional copper wires [16]. This property lets planar transformers operate at very high frequencies, which can give them good performance even without an iron core, resulting in reduced weight and bulk [17]. As a result of these benefits, planar transformers have become very popular in high frequency power electronic converters [16].

The inductances and the coupling factor of the transformer is dependent on its geometry and the core's permeability. Furthermore, the inductances and the coupling factor are linked to each other according to

$$M = k\sqrt{L_1 L_2} \tag{7}$$

where M is the mutual inductance, k is the coupling factor and L_i are the self inductances. A method of calculating the self and mutual inductance of circular spiral coaxial coils in air from their geometry, comparable to finite-element approximation in accuracy, is presented in [18]. For the sake of brevity, the method will not be described here.

2.7 Overcurrent protection

Introduction of air bubbles in a dielectric liquid creates a risk of arcing, where none would exist with purely dielectric liquid between two electrodes [19]. To protect the
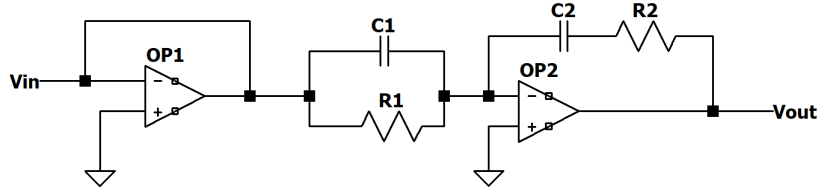
Figure 4: OP-amp PID controller

circuit from any arcs, additional circuitry is used. Active components, such as various switching devices, are commonly used to protect against arcing and overcurrents in electrical power applications [20]. Passive components are an alternative which is more popular in applications other than electrical power. For instance, a resistor can be connected in series with the load, to limit the current in case of an arc [21].

According to APR, a typical arc in their application lasts for 1 μs and has a resistance of 50 Ω.

2.8 OP-amp based PID controllers

To ensure that a system's output converges towards a reference value, a controller such as a PID can be utilised. The most common approach to implementing a PID controller is by using a microprocessor that adjusts the system's input according to equation 8. However, there are alternative ways to implement a PID controller, and one method described in [22] is a purely analogue controller consisting of operational amplifiers. The circuit shown in figure 4 produces the transfer function in equation 9, which shares great similarities with equation 8. The purpose of OP1 is to provide the controller with high input impedance and invert the signal, so that it has a positive sign after being inverted again by OP2.

$$G_c(s) = sK_d + Kp + \frac{K_i}{s} \tag{8}$$

$$G_c(s) = sC_1R_2 + \frac{C_1R_1 + C_2R_2}{C_2R_1} + \frac{1}{sC_2R_1} \tag{9}$$

3 Existing converter topologies

This chapter presents high voltage DC/DC converter topologies of interest, i.e. those which are used in circuits that are close to fulfilling the requirements presented in chapter 1.2. The topologies are either from previous work of APR or from scientific articles.

3.1 Royer-based converter

This topology utilises a Royer oscillator with a transformer to invert and increase the input voltage, which is then further increased by a voltage multiplier bridge and then

rectified. This type of converter has previously been used by APR to power their EHD pumps.
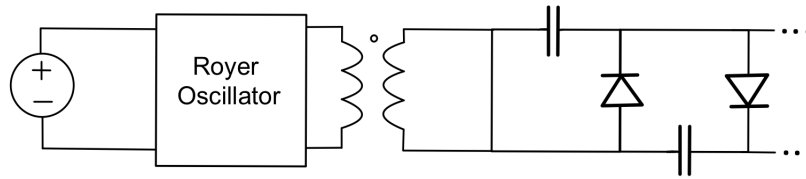
Figure 5: Royer oscillator with transformer connected to a voltage multiplier bridge.

3.1.1 24V to 2.5kV converter used by APR

The circuit in figure 6 is based upon the topology shown in figure 5 and is used by APR to convert 24 V to 2.5 kV while powering a 420 mW load. APR have noted some challenges with this circuit. Firstly, the transformer needs to be specially manufactured for the application which increases costs. Secondly, the circuit lacks a feedback loop, which results in output variations due to the temperature dependence of the transistors. Moreover, the circuit's sensitivity to input voltage fluctuations necessitates the use of a costly linear voltage regulator for stable operation. These challenges highlight areas for potential improvement in the design.

Figure 6: Royer based DC/DC converter used by APR to convert 24 V to 2.5 kV

9

The total cost of the current design is estimated to be 6.5 € of which the transformer contributes with 1.34 €. The transformer utilises an ER 9,5/5 core that is chosen to transfer 0.5 W of power. The mentioned core weighs around 0.6 g and its dimensions are $9.5 * 5 * 5$ mm [23].
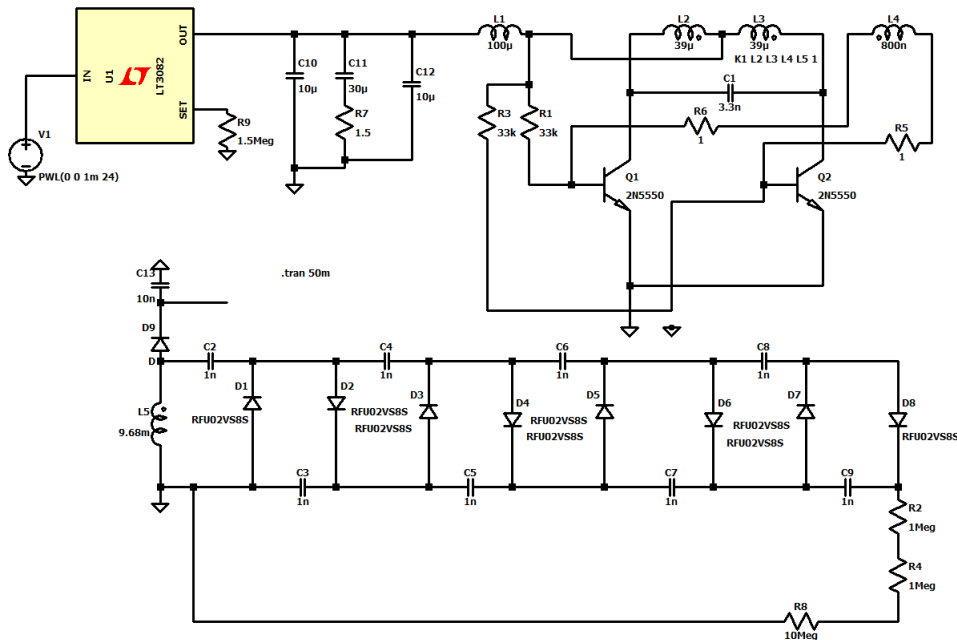
3.2   Transformerless converter

In this topology, the DC input voltage is first increased with a boost converter and then inverted. The AC from the inverter is then connected to a capacitor-diode voltage multiplier, which further increases and also rectifies the voltage. The main benefit of this design is that is that it does not require a transformer for the initial voltage increase, which can be expected to reduce the weight and size of the converter.

One article that investigated this topology showed that it can be used to to convert 5 V to 6 kV while powering a 1 W load [24]. The same method has also been used another article to convert 5 V to 1.5 kV while powering a 2.5 W load [25]. Both of these articles utilised the step-up boost converter LT1618 in series with combined boost converter and inverter LT8331 connected to a Crockcroft-Walton voltage multiplier bridge as in figure 7.
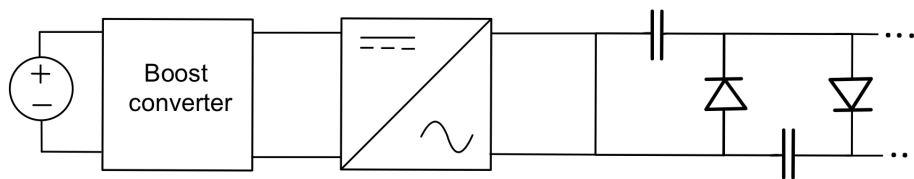
Figure 7: Converter topology consisting of a boost converter followed by an inverter followed by a voltage multiplier bridge.

3.3   Inverter to planar transformer

This topology uses a high frequency inverter to feed a planar transformer integrated into the PCB. Either a voltage multiplier bridge or a rectifier can be used as an end stage [17], [26], [27]. The transformer gives the advantage of reducing the number of multiplier stages, which reduces losses and the number of components. As discussed in chapter 2.6, the high frequency of the inverter makes the transformer efficient, despite being air cored. However, note that iron cored transformers are also used in PCB transformers [28].

Figure 8: Converter topology consisting of a high frequency inverter, followed by a planar transformer that is integrated in a PCB. It can be connected either to a rectifier or a voltage multiplier bridge [17], [26], [27].

4 Method

4.1 Implementation

The topologies from chapter 3 were implemented in LTspice by using the circuit schematics from the articles referred to in chapter 3 as inspiration. For the cases where no schematic was provided, the circuits were created from scratch based on previous knowledge combined with a process of t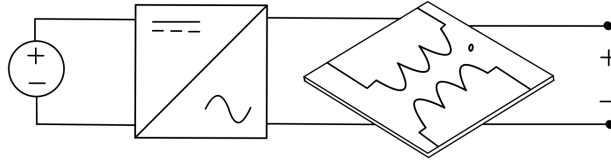rial and error. One exception was made for the Royer-based converter in chapter 3.1, as APR were able to provide a model of a design using this topology. Models of real components that were either included in LTspice or downloaded from component vendors, were used in all circuit models.

4.2 Optimisation

After being implemented, the spice models were altered to optimise their performance, so that they better fulfilled the requirements in chapter 1.2. To do this, one approach was to replace components with more cost-effective or high performance alternatives. Another approach was to alter the operating principle of the circuits through an experimental process of trial and error. Lastly, an approach of combining parts of different topologies was used.

4.3 Evaluation

The simulated circuits were evaluated according to the criteria given in chapter 1.2. Requirements 1–5 were verified with built-in functions in LTspice. This was done by modelling the load as a resistor that was adjusted until it consumed 1.5 W. The circuits were simulated with various input voltages in the range of requirement 1. However, components were chosen for the case of 24 V input voltage and 2 kV output voltage. This case was therefore tested for every circuit. Simulations for the temperatures $-40\,°C$, $0\,°C$, $40\,°C$ and $80\,°C$ were also made, with a 24 V input voltage and a 2 kV output voltage. To verify requirement 6, regarding price, a bill of materials was created in excel (see appendix A.1, A.2 and A.3). Requirements 7 and 8 regarding weight and physical size were verified by creating PCB designs of the circuit.

4.4 Final circuits

Three different circuits were chosen for further evaluation: a feedback-controlled version of the conventional Royer-based converter used by APR, a high frequency Royer-based converter with a planar transformer and a transformerless converter.

4.4.1 Conventional Royer-based converter

The conventional Royer-based converter was created from the topology described in chapter 3.1 and specifically from APR's previous design. Figure 9 shows the new circuit. The circuit was altered by replacing a linear voltage regulator IC (LT3082) with a new discrete voltage regulator. The benefit of the discrete voltage regulator is that it is controlled though a feedback loop from the output of the regulator. This feedback was intended to do two things: (a) ensure that the output converged towards the same value for a range of input voltages and temperature, (b) compensate for deviations within the load or in any of the components. A four-stage Cockroft-Walton bridge was used.
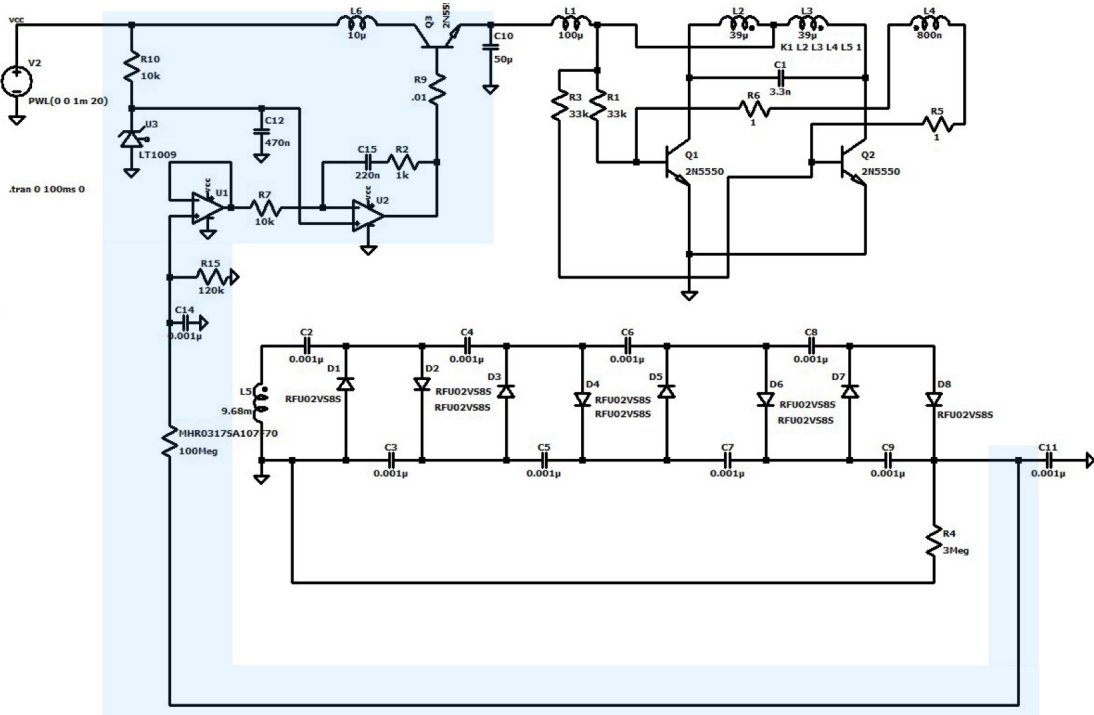
Figure 9: Conventional Royer-based converter with feedback. The feedback loop is highlighted in blue. The rest of the circuit consists of a Royer oscillator with a ferrite core transformer and a Cockroft-Walton bridge. A larger version of the figure can be found in appendix A.1

The feedback circuit regulated the input voltage of the oscillator by using the NPN transistor 2n5550 to control the current that was supplied to the circuit. The transistor was controlled by an OP-amp based PI-regulator, as described in chapter 2.8. The PI-regulator used a 2.5 V reference from the bandgap voltage reference LT1009. The spe-

cific coefficients of the PI-regulator were found through trial and error. Due to a lack of time, no PCB design was created for this circuit.

4.4.2 High-frequency Royer-based converter

The converter design presented in figure 10 is a variant of the the conventional Royer-based converter presented above, in chapter 4.4.1. Instead of BJTs, GaN-tansistors (EPC8010) were chosen to allow the oscillator to operate at high frequency, enabling the use of a planar air-core transformer (see chapter 2.6), instead of a conventional transformer. The PCB is shown in 11.
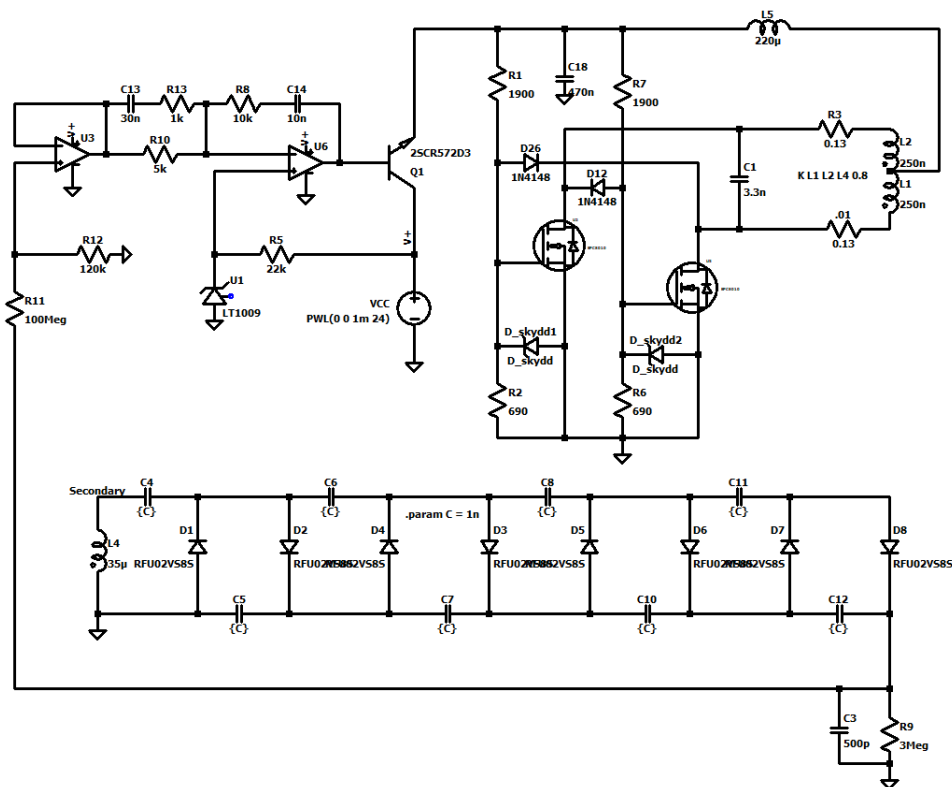
Figure 10: Royer-based converter utilising a planar PCB transformer with an air core, connected to a Cockroft-Walton voltage multiplier. A larger version of this figure can be found in appendix A.1.

The design of the transformer was governed by the size requirements presented in chapter 1.2 – the secondary side's outer diameter being limited by the absolute maximum of 3 cm. Note that the PCB substrate was extended beyond the edge of the transformer to prevent arcing. Furthermore, resistive losses and the coupling factor of the transformer were major factors in the design. The PCB that was created was used to calculate the resistance of the transformer windings from the width, length and depth of the copper traces. To allow for wider traces and thus a lower winding resistance while retaining the number of turns, the secondary coil was split in two equal parts which were put in

PCB layers next to each other. Thus, the transformer's layers were: secondary winding first half (top), secondary winding second half (middle), primary winding (bottom). The transformer's theoretical coupling factor as well as its self- and mutial inductances were calculated with equation 7 and with the method mentioned in chapter 2.6, to be $L_1 = 570\,\text{nH}$, $L_2 = 42\,\mu\text{H}$, $M = 3.9\,\mu\text{H}$ and $k = 0.80$. ND was set to 10 for an accuracy of 0.1 % according to the creators of the method. Dimensions and calculated quantities are presented in table 1.

Table 1: Planar PCB transformer parameters and calculated self-inductances. The mutual inductance and the coupling factor were calculated to $3.9\,\mu\text{H}$ and 0.80, respectively.

	Primary coil	Secondary coil
Number of turns	5	26
Outer radius [mm]	15	15
Inner radius [mm]	6	6
Copper thickness [µm]	70	35
Substrate thickness [mm]	1.6	1.6
Self-inductance [µH]	0.57	42

Note that this circuit used the same type of PID-controlled linear voltage regulator as the conventional Royer-based converter in chapter 4.4.1.
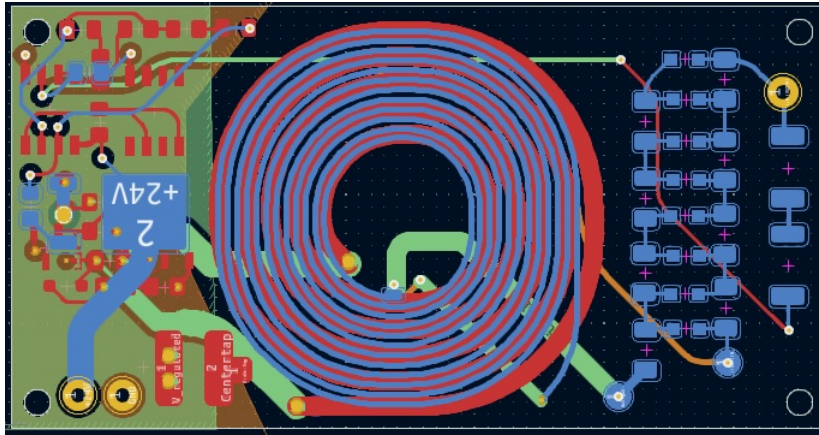
Figure 11: PCB layout of the high frequency Royer converter. The circular traces make up the planar transformer. The red trace is the primary winding placed on the front of the PCB. The blue trace makes up half of the secondary winding and is placed on the back of the PCB. The other half of the secondary winding (not visible) is placed directly under the blue trace on a inner layer of the PCB. The dimensions of the PCB are $6.3 * 3.3\,\text{cm}$.

4.4.3 Transformerless converter

The transformerless topology incorporated an LT8331 switching boost converter and a Cockroft-Walton voltage multiplier. The voltage multiplier was arranged according to the series-connected positive-negative voltage multiplier layout described in chapter 2.4.2. To minimise the voltage drop in the multiplier, the boost converter was configured to operate at its maximum frequency of 500 kHz.

To closer meet the safety standard [29], section 6 "Protection against electric shock", the capacitors in the Cockroft-Walton bridge were chosen to have to largest possible capacitance while not exceeding a total charge of 45 µC. The total charge was calculated as follows

$$Q = \hat{U}_{in} \cdot C \cdot N_C \cdot 1.1 \tag{10}$$

Where $\hat{U}_{in}$ is the peak pulsating voltage entering the voltage multiplier, C is the capacitance used for every capacitor, N_C is the total amount of capacitors in the bridge and the constant 1.1 represents the capacitors maximum tolerance of 10 %.

A target value of 112 V was chosen as the output voltage from the LT8331, in order to have a 20 % safety margin to the stated absolute maximum output voltage of 140 V. Equation 1 therefore gives 18 as the number of stages to reach an output voltage of 2 kV.

It was then found through simulation that 22 stages were necessary to reach an output voltage of 2 kV, when adjusted for the maximum allowed charge in the voltage multiplier previously stated. The input voltage to the bridge, i.e. the output voltage from the LT8331, was then found to be 111 V (see figure 20). Thus, equation 10 gives

$$C = \frac{Q}{\hat{U}_{in} \cdot N_C \cdot 1.1} \approx 8.6\,\text{nF} \tag{11}$$

The E12 value of 8.2 nF was therefore chosen. This resulted in a total charge of approximately 42.7 µC. The final circuit is shown in figure 12.

This was then compared to equation 3, which takes voltage drop into consideration and 22 stages were found necessary to reach 2kV, which was expected. (Note that when applying equation 3 to the Series positive-negative voltage multiplier you half the stages, taking into consideration only one of the parallel voltage multiplier and then multiply the output voltage by 2 to get an accurate result.)
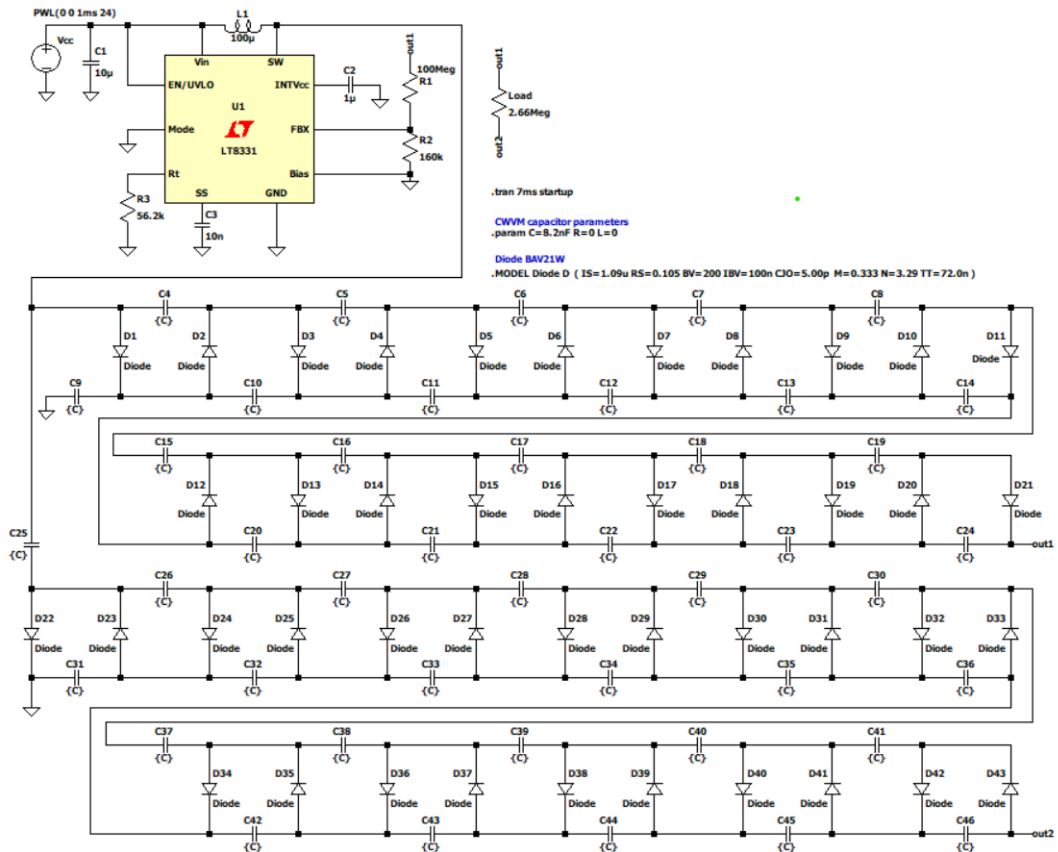
Figure 12: Boost converter combined with a 22 stage series-connected positive-negative Cockroft-Walton voltage multiplier.

An alternative choice of capacitors in the Cockroft-Walton bridge was made according to the optimised scheme described by equation 4 in chapter 2.4.1. The capacitors chosen were E12 values between 1.5 nF and 15 nF. The total stored charge of this bridge, calculated with 110 V over each capacitor, was approximately 37 μC.

A PCB was designed for the circuit with capacitors of equal capacitance. Its layout is shown in figure 13.
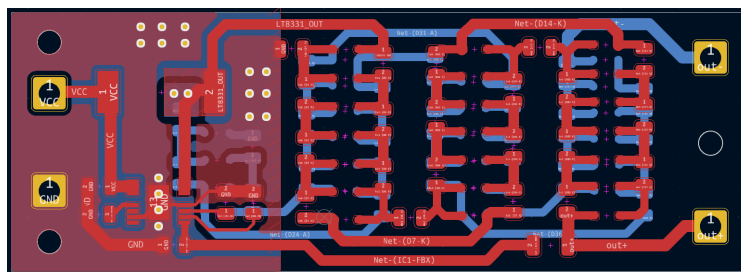
Figure 13: PCB layout of the transformerless DC-DC converter. The PCB is made up of a two layer board with the dimensions 6.21 cm ∗ 2.21 cm

16

4.4.4 Overcurrent protection

To protect against overcurrent without adding significantly to the circuits' losses, components such as Transient-voltage-suppression (TVS) diodes and varistors were considered. However, due to the high cost of components with the necessary voltage rating, such a solution was not possible to implement. Instead, series inductances and resistances ($100\,\text{k}\Omega$ and $1\,\text{M}\Omega$) were tested. The inductance value was increased from $1\,\text{µH}$ until the simulation showed that the goal in 1.2 was fulfilled.

Arcing was tested through simulation in LTspice, by the use of a switch which was connected in parallel with the load. The switch was on for $1\,\text{µs}$ and had an on resistance of $50\,\Omega$, in accordance with the arcing case described in 2.7. Its rise and fall times were $1\,\text{ns}$ respectively. Simulations were done with the conventional Royer-based converter and the transformerless converter. The high-frequency Royer-based converter was not used, since its voltage multiplier was the same as the one used in the conventional Royer-based converter.

5 Results

The three different circuits described in chapter 4.4 all fulfilled requirements 1–5 presented in chapter 1.2, except for requirement 4. With an input voltage of $24\,\text{V}$, the conventional converter had an efficiency of $50\,\%$, the high-frequency converter $58\,\%$ and the transformerless converter $91\,\%$. The LTspice circuit schematic and bill of materials for each converter is presented in appendix A.1, A.2 and A.3.

5.1 Conventional Royer-based converter

The circuit presented in chapter 4.4.1 was estimated to cost $7.03\,€$. Its switching frequency was circa $191\,\text{kHz}$ for every test case. The sum of the components' weight was $3.2\,\text{g}$.

Simulation was done with the standard voltages and temperatures presented in chapter 4.3. After $100\,\text{ms}$, the output voltage had stabilised to circa $2\,\text{kV}$ for each temperature. The efficiency of the circuit was almost unaffected by temperature. The results can be seen in figure 14.

Figure 14: Output voltage for $-40\,°C$, $0\,°C$, $40\,°C$ and $80\,°C$ from the Royer-based converter in figure 9. The efficiency was almost unaffected by temperature.

The circuit was also simulated with the input voltages $20\,V$, $22\,V$, $24\,V$ and $26\,V$, where the temperature used was the LTspice standard temperature of $27\,°C$. After $100\,ms$, the output voltage had stabilised to circa $2\,kV$ for each input voltage. The efficiency varied between $46\,\%$ and $78\,\%$. The inputted power that was not outputted was mainly dissipated in the feedback loop. These results can be seen in figure 15 and table 2.

Table 2: Characteristics of the conventional Royer-based converter at $27\,°C$ for four input voltages. For every case, the switching frequency was $191\,kHz$ and the cost of the circuit was $7.06\,€$.

Input voltage [V]	20	22	24	26
Steady state V_{out} [V]	2078	2082	2084	2086
Efficiency [%]	60	54	50	46
P_{out} [W]	1.440	1.447	1.449	1.451

(a) With voltage regulation.

(b) Without voltage regulation.
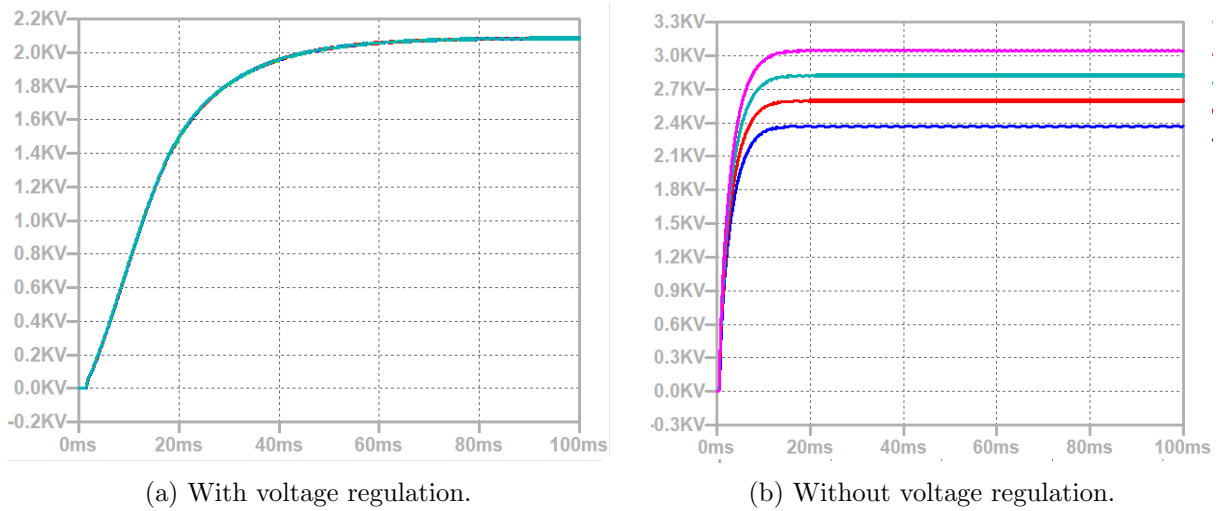
Figure 15: Output voltage for input voltages 20 V, 22 V, 24 V and 26 V from the Royer-based converter in figure 9 with and without voltage regulation.

5.2 High-frequency Royer converter utilising a planar transformer with an air core

The circuit presented in 4.4.2 was estimated to cost 7.02 € and it weighed ca 10 g. Its switching frequency was circa 2.8 MHz for every test case.

After 5 ms of simulation under the standard conditions described in chapter 4.3, the circuit's output voltage had stabilised to circa 2 kV for each case. The efficiency of the circuit was almost unaffected by temperature. See figure 16 for these results.
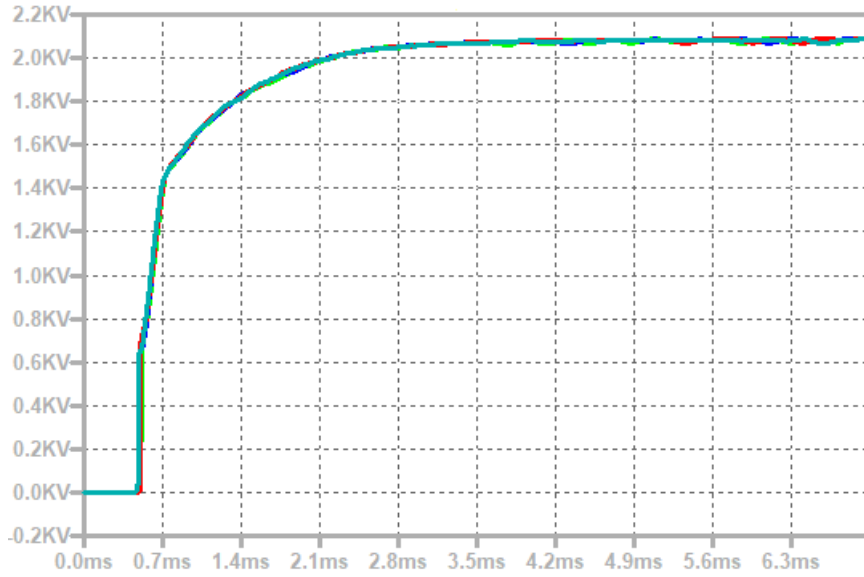
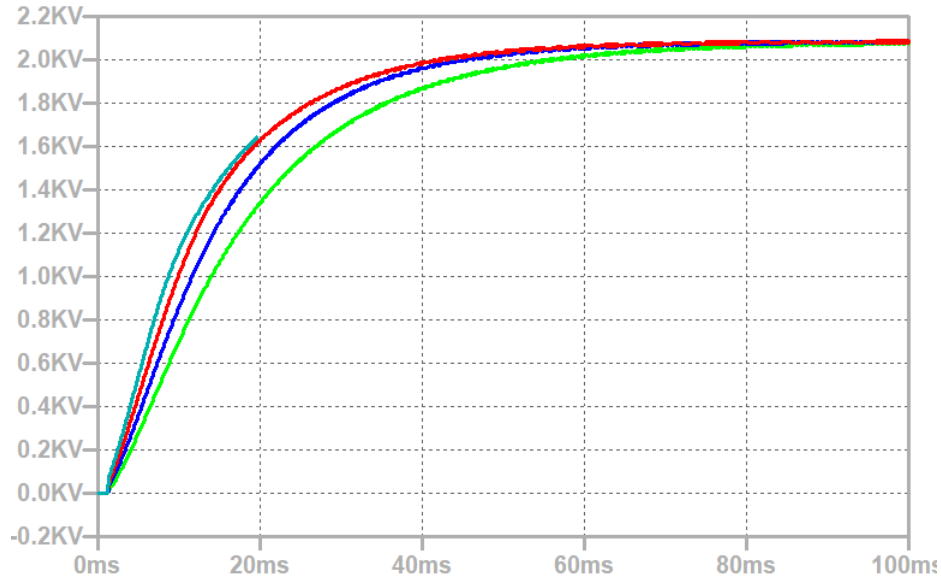Figure 16: Output voltage for $-40\,^{\circ}\mathrm{C}$, $0\,^{\circ}\mathrm{C}$, $40\,^{\circ}\mathrm{C}$ and $80\,^{\circ}\mathrm{C}$ from the high frequency Royer-based converter in figure 10. The efficiency was almost unaffected by temperature.

The input voltages $16\,\mathrm{V}$, $18\,\mathrm{V}$, $20\,\mathrm{V}$, $22\,\mathrm{V}$, $24\,\mathrm{V}$ and $26\,\mathrm{V}$, were also used to test the circuit in simulation. For these cases, the LTspice standard temperature of $27\,^{\circ}\mathrm{C}$ was used. An output voltage of circa $2\,\mathrm{kV}$ was reached for every input voltage after circa $5\,\mathrm{ms}$. The efficiency of the circuit was between $40\,\%$ and $75\,\%$. The power delivered to the load was $1.45\,\mathrm{W}$ for each input voltage except $16\,\mathrm{V}$, for which it was $1.24\,\mathrm{W}$. Table 3 and figure 17 shows these results.

Table 3: Characteristics of the Royer air core converter for six input voltages, at $27\,^{\circ}\mathrm{C}$. The cost of the circuit was $7.02\,\text{\euro}$ for every case. Its switching frequency was $2.8\,\mathrm{MHz}$ for every case.

| Input voltage [V]	16	18	20	22	24	26
Steady state V_{out} [V]	2002	2082	2084	2086	2086	2088
Efficiency [%]	68	60	56	48	45	41
P_{out} [W]	1.24	1.45	1.45	1.45	1.45	1.45
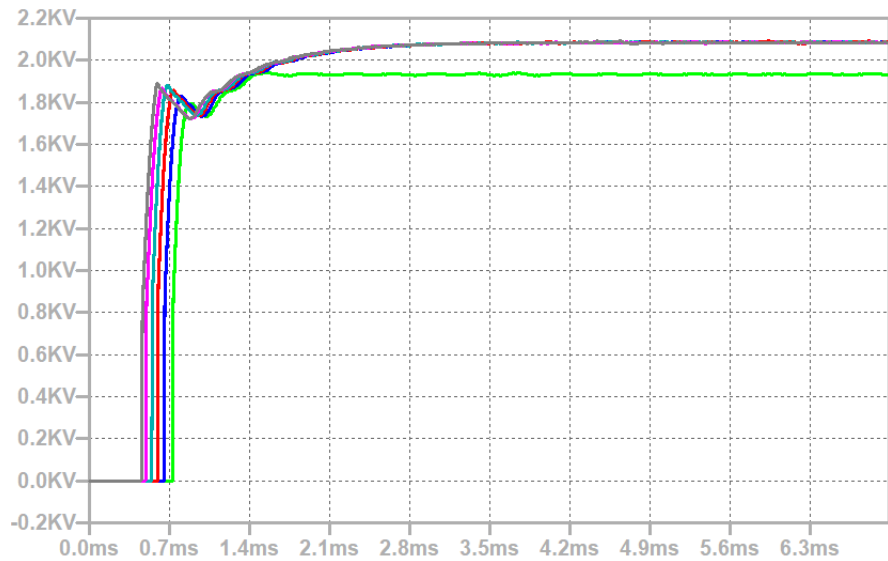
Figure 17: Output voltage for input voltages 16 V, 18 V, 20 V, 22 V, 24 V and 26 V from the high-frequency Royer converter in figure 10.

5.3 Transformerless converter

The circuit presented in 4.4.3 was estimated to cost 10.4 € with all capacitors having a capacitance of 8.2 nF. The circuit's weight was circa 9 g. With the optimised bridge, the circuit was estimated to cost 10.6 €. The switching frequency was circa 500 kHz for every test case and both variants of the circuit.

In figure 18 the output voltage and rise time is compared for temperatures ranging from −40 °C to 80 °C. The rise time was circa 2.8 ms for each temperature. All the temperatures were tested with a 24 V input voltage. The efficiency of the circuit was also almost unaffected by temperature.
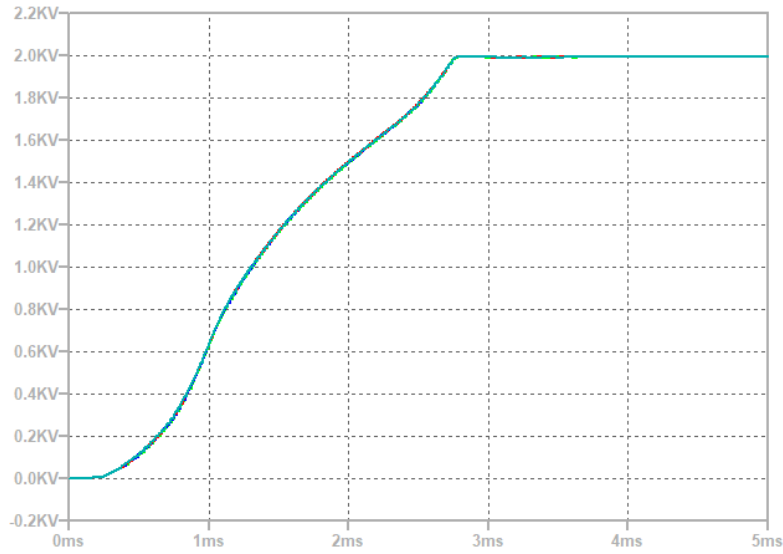
Figure 18: Output voltage for temperatures $-40\,°C$ (pink), $0\,°C$ (turquoise), $40\,°C$ (red) and $80\,°C$ (blue) from the DC-DC converter in figure 12. The input voltage was $24\,V$ for every temperature text

Both variants of the circuit were simulated with the input voltages $12\,V$, $24\,V$, $36\,V$ and $48\,V$, at the LTspice standard temperature of $27\,°C$. After $4\,ms$ of simulation, a steady output voltage of circa $2\,kV$ had been reached. The efficiency varied between $55.79\,\%$ and $91.59\,\%$ for the circuit shown in figure 12, while it varied between $36.46\,\%$ and $89.26\,\%$ for the circuit with the optimised bridge. See figure 19 and table 4 for the results from the converter with equal capacitances and see table 5 for the results from the converter with optimised capacitances.
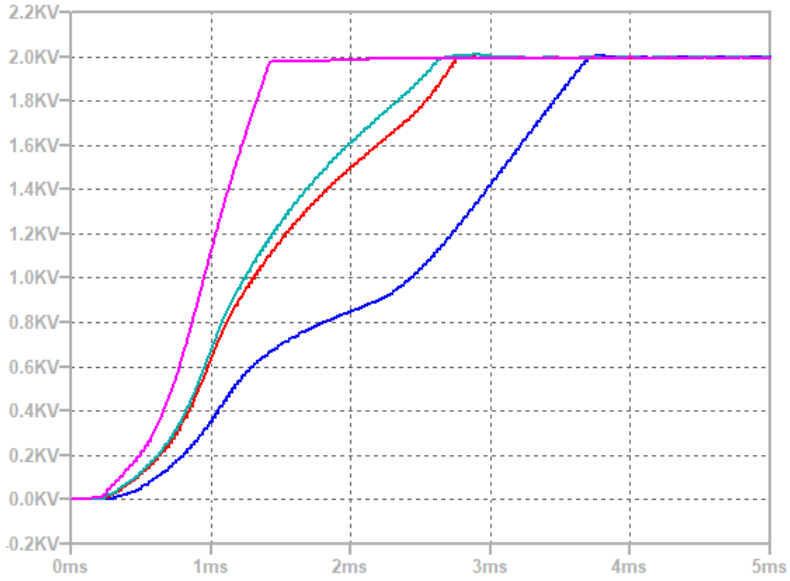
Figure 19: Output voltage for input voltages 48 V (pink), 36 V (turquoise), 24 V (red) and 12 V (blue) from the DC-DC converter in figure 12.

Table 4: Characteristics of the LT8331 Cockroft-Walton DC-DC converter circuit seen in 12 during four different input voltages. For every case, the switching frequency was 500 kHz. The standard temperature in LTspice of 27 °C was used for every case.

Input voltage [V]	12	24	36	48
Steady state V_{out} [V]	1979	1976	1978	1975
Efficiency [%]	55.79	91.59	90.09	82.04
P_{out} [W]	1.472	1.469	1.471	1.467
Output ripple. [V]	2.799	1.976	1.977	1.836

Table 5: Characteristics of the LT8331 Cockroft-Walton DC-DC converter circuit seen in 12, except with bridge capacitances optimised according to the scheme described in equation 4. The standard temperature in LTspice of 27 °C was used for every case.

Input voltage [V]	12	24	36	48
Steady state V_{out} [V]	2008	2002	2004	2002
Efficiency [%]	36.46	87.42	89.26	81.81
P_{out} [W]	1.494	1.485	1.487	1.484
Output ripple [V]	4.306	3.856	2.609	2.793

23

The voltage stress of the capacitor-diode stages in the CWVM used in the proposed transformerless converter can be seen in 20. The figure shows the Series-connected positive-negative voltage multiplier (SPNVM) which generates the negative voltage, the SPNVM generating the positive voltage can be assumed to have the same voltage stress. The first stage in red can be shown to have a voltage stress slightly lower than the pulsating input voltage of 110 V. A lower voltage stress is observed on the sixth stage in green and the last (eleventh) stage in blue.
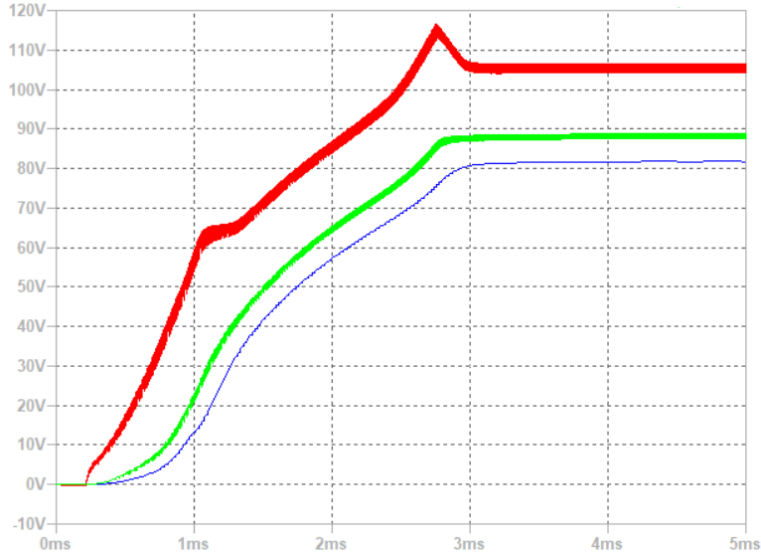
Figure 20: Voltage stress over capacitor-diode stages in the Cockroft-Walton voltage multiplier generating negative voltage. First stage (red), sixth stage (green), eleventh and last stage (blue).

5.4 Overcurrent protection

Only the conventional Royer-based converter fitted with a 1 MΩ series resistance and a 1 H series inductances had a peak output current below the goal of 2 mA.

For the conventional Royer-based converter, the results are presented in table 6. The lowest peak output current was achieved for the circuits with a 1 MΩ series resistance and 1 H series inductance, which reached 1.9 mA of output current.

For the transformerless converter, the results are presented in table 7. No combination of components resulted in the goal being achieved. The lowest peak output current was achieved for the circuit with a 1 MΩ series resistance and 1 H, which reached 2.5 mA in output current.

Table 6: Peak output current from the conventional Royer-based converter while arcing, for various values of series suppression components.

Inductance	$\hat{I}_{out}$ (R=100 kΩ) [mA]	$\hat{I}_{out}$ (R=1 MΩ) [mA]
1 µH	21	2.6
10 µH	21	2.6
100 µH	21	2.6
1 mH	21	2.6
10 mH	16	2.6
100 mH	13	2.6
1 H	2.6	1.9

Table 7: Peak output current from the transformerless converter while arcing, for various values of series suppression components.

Inductance	$\hat{I}_{out}$ (R=100 kΩ) [mA]	$\hat{I}_{out}$ (R=1 MΩ) [mA]
1 µH	22	3.5
10 µH	22	3.5
100 µH	22	3.5
1 mH	22	3.5
10 mH	22	3.5
100 mH	14	3.4
1 H	2.9	2.5

6 Discussion

6.1 Conventional Royer-based converter

The conventional Royer-based converter fulfilled each of requirements 1–6, except requirement 4 regarding efficiency. The low efficiency was mainly due to the linear regulation of input voltage, the usage of which was motivated by the fact that a switched regulator was thought to be too complex and expensive for this application.

Since no PCB was designed for the circuit, requirement 7 regarding size could not be thoroughly verified. However, due to the circuit's similarity to the high-frequency Royer-based converter, except for the large planar transformer, it is reasonable to assume that a PCB could be designed to be within the size limits. The total weight of the components was circa 196.8 g lower than the weight limit specified in requirement 8, therefore it is highly likely that the weight requirement would also be fulfilled. Thus, it can be concluded that the conventional Royer-based converter fulfilled every requirement except requirement 4.

6.1.1 PID-feedback

Based on figures 14 and 15a it can be concluded that the feedback effectively eliminated output variations for a range of temperatures and input voltages. The total cost of the components in the feedback loop was 2.4 € which is identical to the cost of the linear voltage regulator LT3082 that was used in APR's design. It can be concluded that this is a clear improvement in the design. In applications where price is more important than robustness, it is also possible to use the Royer-based converter without any voltage regulation. This does however result in large variations in output voltage, as seen in figure 15b.

6.2 High-freqency Royer-based converter

The high-frequency Royer-based converter fulfilled all requirements, except requirement 4 regarding efficiency and requirement 7 regarding size. The efficiency requirement was not met for the same reason as for the conventional Royer-based converter, i.e. that the circuit utilised linear voltage regulation. The size requirement was not met due to the transformer having an outer diameter of 3 cm, which required the PCB substrate to extend beyond the size requirement of 3 cm in width. However, as the PCB was shorter than required, the total area of the converter was $20.8\,\text{cm}^2$, i.e. $9.2\,\text{cm}^2$ smaller than the limit dimensions result in. To reduce the width of the PCB, the shape of it could be changed to be more oval. This would however make the calculation of the inductances considerably more difficult. Alternatively one turn could be removed from each half of the secondary coil or the width of the traces and/or the distance between the traces could be reduced. But, these changes would lower secondary inductance and lower the breaktrough voltage, respectively.

6.2.1 Planar air-core transformer

As was mentioned in chapter 2.6, the main benefits of planar transformers is that they increase repeatability while reducing weight, bulk and cost. As was mentioned in chapter 3.1.1, the transformer that was used in APR:s initial design was chosen to transfer 500 mW while weighing 0.6 g and having the dimensions $9.5 * 5 * 5$ mm. If the assumption is made that the core can transfer 1.5 W if it is scaled up so that is has thrice the volume, it would then have the dimensions $13.7 * 7.2 * 7.2$ mm while weighing 1.8 g. The surface area that this transformer would occupy would still be less than the $30 * 30$ mm required by the planar air core transformer. It is possible that the area occupied by the planar air-core transformer can be shared with other components but it is unclear how they would be affected by the electromagnetic fields from the transformer, especially as the transformer is completely unshielded. Placing components on top of the planar air-core transformer was not tested in the PCB-layout in figure 11, as the risk of EMI issues was deemed to be too great. A conclusion that can be drawn from this, is that a planar air-core transformer can reduce the profile of the circuit, but requires much more surface area than a conventional transformer.

From a cost perspective the transformer was practically negligible, but the high frequency required, along with the demands on rated current, made the use of GaN-transistors

necessary. These had a combined cost of 1.96 € which is slightly more than the cost of the conventional transformer. From this, the conclusion can be drawn that the planar transformer was not beneficial in terms of price.

To summarise the two paragraphs above, it can be said that the planar air core transformer did not prove beneficial, neither in regards to price nor size. As the iron core required for 1.5 W power transfer was assumed to weigh only 1.8 g, it can be concluded that the benefit of potential weight decrease is also not relevant in this application.

A possible improvement could be to utilise a planar transformer with an iron core, as in figure 21. This would not reduce weight. However, it would still replace the copper windings with PCB-traces, thus keeping the benefits of increased repeatability and reduced manufacturing costs. It is also likely that it would greatly reduce the required footprint area as the transformer can achieve the same inductance with fewer windings. It would also be possible to lower the circuit's frequency, which would allow the use of conventional MOSFET:s instead of GaN-transistors, thus reducing cost.
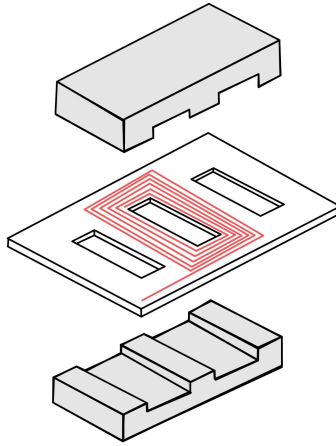

Figure 21: Planar transformer with iron core

The transformer could also be improved by placing the primary coil between the halves of the secondary coil, instead of having both halves of the secondary coil on the same side. This would increase the coupling factor which should increase the efficiency of the transformer. The inductance of the secondary coil would, however, be slightly lowered. Note that if an iron core is used, the coupling factor would be close to 1, regardless of whether this change is made. Thus, the geometry used in this report would be beneficial to retain, in order to keep the higher secondary side inductance.

6.3   Transformerless converter

For the input voltages 24 V, 36 V and 48 V, the transformerless converter fulfilled every requirement, except the one regarding price (requirement 6). The circuit performed best with an input voltage of 24 V with an efficiency of 91.59 % and a voltage ripple of 1.469 V resulting in a ripple factor of 1 %. The circuit performed equally well with

an input voltage of 36 V. With 48 V input voltage a decrease in efficiency was noted but the circuit still met the efficiency requirements. When the circuit was fed with 12 V however, the efficiency was greatly decreased, dropping to an efficiency of 55.79 % and thereby not meeting the efficiency stated in requirement 4. A hypothesis for the low efficiency is the extra stress from the high conversion ratio required for the boost converter to operate from 12 V. Taking this into consideration, it would be reasonable to recommend an input voltage of 24 V–48 V and for lower input voltages that an additional boosting stage should be used before the LT8331 circuit to increase efficiency.

6.3.1 Series-connected positive-negative voltage multiplier

The application of the series-connected positive-negative voltage multiplier (SPNVM) offers significant advantages over a conventional Cockroft-Walton voltage multiplier. The SPNVM allows for the use of very low capacitance, meeting the maximum charge requirements specified in [29]. Additionally, it enables the achievement of high gain, low voltage ripple and minimal voltage drop, which would have been challenging to achieve with a traditional Cockroft-Walton voltage multiplier.

During the testing phase, it was observed that a conventional Cockroft-Walton voltage multiplier failed to operate effectively due to excessive voltage drop caused by the low capacitance in the bridge used in order the meet the maximum charge requirements. This resulted in the LT8331 surpassing its absolute maximum switching voltage of 140 V.

The SPNVM's low ripple factor eliminated the need for an output capacitor, which is typically required in a conventional Cockroft-Walton voltage multiplier to reduce the ripple when multiple stages are employed. The specification for such an output capacitor would need to accommodate the high voltage stress of the entire output voltage (2 kV), potentially resulting in a bulky component within the otherwise compact PCB utilised in the proposed transformerless converter.

Finally, it is important to note that the SPNVM produces both a positive voltage 1 kV and a negative voltage −1 kV, rather than the conventional single-ended 2 kV to ground connection. This distinction must be taken into consideration when connecting the EHD-pump.

6.3.2 Optimised Cockroft-Walton voltage multiplier

The circuit with the optimised voltage multiplier performed worse than the one with capacitors of equal capacitance, in terms of both efficiency and output ripple. This was likely due to the fact that the bridge with equal capacitances had a larger total capacitance, compared to the optimised bridge. Furthermore, the optimised bridge had a higher cost and complexity, due to the many different capacitors needed. Since the voltage multiplier with equal capacitances outperformed the optimised one, while not exceeding the limit of 45 μC in total charge, it can be concluded that the circuit with equally large capacitors is the better choice.

It is possible that an optimised bridge could outperform a bridge with equal capacitances, if their total capacitances were equal. This could be an area of further research,

for applications where ripple and efficiency is more important, while the requirement on total charge is more limiting. Note however, that the method of optimisation mentioned in 2.4.1 considers a regular Cockroft-Walton bridge, not a series-connected positive-negative one.

6.3.3   Cost reduction

One major drawback of the circuit is its relatively high cost due to the presence of the boost converter LT8331 and the large voltage multipliers. Consequently, the transformerless converter presented in this report may not necessarily be a cheaper alternative to a circuit with a transformer.

However, there is potential for cost reduction by exploring alternative choices for capacitors and diodes, as these make up the majority of components used in the circuit. The capacitors deviate from commonly used specifications, and slight adjustments to their values, either up or down, could potentially lead to a reduction in cost.

Among the components, the LT8331 boost converter stands out as the most expensive single part – accounting for nearly half of the total cost. Thus, finding a more affordable replacement would be beneficial, but no suitable IC was found during the course of this investigation. Alternatively, designing a suitable boost converter instead of buying an IC could be considered, but that would not necessarily be a more affordable solution.

6.3.4   Manufacturing dependency

A drawback of the proposed circuit in section 4.4.3 is the use of the boost converter LT8331 to solve the vital part of generating the square wave for the voltage multiplier. This results in a dependence on Analog Circuits to supply the boost converter. Considering the shortage of semiconductors in recent years, if the proposed circuit is to be put in production there is a dangerous supply line risk if Analog Circuits were to stop producing or drastically changing the price of the boost converter.

A solution to this would be to design a new switching boost converter from scratch instead of using the LT8331. This would result in a more reliable manufacturing process were the supply line is not dependent on one single circuit. But considering the LT8331's good performance and ability to boost, switch and provide a voltage feedback it might be a complicated and costly task to design a circuit to match its performance. As stated above in chapter 6.3.3, finding an alternative IC could also be beneficial, but no such circuit was found during this investigation.

6.4   Comparison

Both of the converters with a Royer oscillator performed well for input voltages close to 24 V, for which they were designed. However, they were surpassed in efficiency by the transformerless converter. It reached 91.59 %, in comparison to 50 % for the conventional Royer-based converter and 45 % for the high-frequency Royer-based converter. Note however, that the Royer-based converters' efficiency increased for lower input voltages, with the conventional Royer-based converter reaching 60 % efficiency for an input voltage

of 20 V and the high-frequency Royer-based transformer reaching the same efficiency for 18 V. The transformerless converter was not tested at these input voltages, but its efficiency could be assumed to be between 91.59 % and 55.79 %. Furthermore, the transformerless converter also performed well for a wider range of input voltages compared to the Royer-based converters. However, this better efficiency and wider operating range comes at the cost of circa 3.4 € in increased cost (an increase of circa 48 %) and the increased risk of dependence on a single manufacturer.

With a broader view, it can be presumed that a Royer-based converter would have a significantly lower cost and a significantly lower efficiency than a transformerless converter similar to the one investigated in this report. Furthermore, if a boost converter is purchased rather than built, a transformerless converter can be presumed to have a greater risk of production disruptions, compared to a Royer-based converter, if these converters are similar to those presented here.

6.5   Overcurrent protection

The desired limit of 2 mA peak output current was only achieved by the 1 MΩ series resistance in conjunction with the 1 H series inductance, and only for the Royer-based converter. An inductor with such a large inductance would add significantly to both the cost and the bulk of each converter in this report.

The transformerless converter had a larger peak output current for every combination of components. This may be explained by the larger capacitance in the circuit.

A series resistance of 1 MΩ was required to limit the output current enough to achieve the goal. The large inductance that was also required could be removed if an even larger resistance was used. However, a 1 MΩ series resistor would already consume

$$P_R = R \cdot I_{out}^2 = R \cdot \left(\frac{P_{out}}{U_{out}} \right)^2 = 10^6 \cdot \left(\frac{1.5\,\text{W}}{2000\,\text{V}} \right)^2 \approx 0.56\,\text{W} \tag{12}$$

and thereby contribute with losses corresponding to a third of the output power.

Since simple series components do not seem to perform well enough, it would be desirable to find an alternative solution. However, using specialised components seems to be prohibited by cost, as stated in chapter 4.4.4. Further research is needed on this subject. Perhaps a varistor or TVS diode could be used together with a voltage divider in parallel with a series connection of the load and an inductor.

7   Conclusions

7.1   Conventional Royer-based converter

The conventional Royer-based converter fulfilled every requirement except requirement 4, regarding efficiency. Compared to APR's converter, replacing the linear voltage regulator IC with a discrete voltage regulator controlled by a feedback loop resulted in better performance at the same cost. The feedback loop made the converter's output

voltage constant for a range of input voltages (20 V–26 V) and a range of temperatures (−40 °C–80 °C). However, it also reduced the converter's efficiency. See chapter 7.5 below for further conclusions on the feedback loop.

This converter had a slightly higher efficiency than the high-frequency Royer-based converter, but a significantly lower efficiency than the transformerless converter. However, its cost was also significantly lower than that of the transformerless converter.

7.2 High-frequency Royer-based converter

The high-frequency Royer-based converter fulfilled all requirements, except requirements 4 and 7, regarding efficiency and size, respectively. The size requirement was exceeded due to the transformer having a diameter equal to the width requirement of the PCB and the extra substrate around its edge. A more oval transformer could make the circuit fit within the size requirements, but would make calculation significantly harder. Alternatively, if worse characteristics are acceptable, the circuit could be made to fulfil the size requirements by reducing the size of the transformer. Like for the conventional Royer-based converter, the feedback made the converter's output voltage stable, but reduced its efficiency.

In comparison to the other converters, this circuit had the lowest efficiency. Although, it was only slightly lower than the conventional Royer-based converter's efficiency. The cost benefits of the planar transformer were undone by the more expensive transistors used to achieve the necessary frequency. Thus, the converter was almost identical in price to the conventional Royer-based converter. For further and more general conclusions on the planar transformer, see chapter 7.4 below.

7.3 Transformerless converter

The transformerless converter fulfilled every requirement except requirement 6 regarding cost, for the input voltages 24 V, 36 V and 48 V. The built-in feedback of the LT8331 switched boost converter used, made the output voltage constant for a range of conditions, like the other converters in this report.

It outperformed the other converters presented in this report in terms of efficiency and range of acceptable input voltages. This was likely due to the LT8331 regulating the voltage through switching, rather than letting the extra energy dissipate in the feedback loop. However, the converter was also more expensive and the requirement of a special IC would make future production more susceptible to disruption. Replacing the LT8331 could reduce cost and production uncertainty, but could also be quite difficult.

The biggest drawback of the circuit was this relatively high cost. The causes of this was the boost converter LT8331 and the large voltage multiplier which used a large number of components with special requirements, making them more expensive than expected. This made the presented transfromerless converter a not necessarily cheaper alternative to a circuit with a transformer.

7.4 Planar transformers

According to chapter 6.2.1 it can be said that planar transformers are cheaper to produce, have a lower profile and have higher production repeatability. However, on the whole they do not have any advantages over conventional transformers in the type of power converters that were analysed in this report. While a planar transformer is cheaper than a conventional one, the GaN-transistors required to achieve high enough switching frequencies are expensive, thus counteracting any cost savings that come from using a planar transformer. The planar transformer also required more area on the PCB than a conventional transformer. Furthermore, the weight savings that come with using it is almost negligible, as a transformer required to transfer 1.5 W would already be very light. The use of iron-cored planar transformers may provide the advantages of lower profile and cheaper production, without the need of very high frequencies. This, however, cannot be concluded from this report and should instead be investigated further.

7.5 PID-feedback

According to chapter 6.1.1, the conclusion can be drawn that a discrete linear voltage regulator controlled by an analogue PID-controller is an effective way to ensure that the output from a power converter remains constant for a large range of temperatures and input voltages. The only drawback found was that linear voltage regulation lowers the efficiency of the converter. The discrete regulator presented in this report was found to be a clear improvement from LT3081 which was previously used in one of APR's converters. In applications where output voltage variations are acceptable, or where constant temperature and input voltage can be guaranteed, it is possible to save costs by not using any voltage regulator.

7.6 Overcurrent protection

From chapter 6.5 it can be concluded that of the tested circuits for overcurrent protection, the only ones which performed well enough were those which used unfeasibly large components. For the combination of resistor and inductor, their values would have to be 1 MΩ and 1 H. A larger resistor could be used in order to do away with the inductor, but already the 1 MΩ resistor would add 0.56 W to the losses.

References

[1] Mikael Antelius et al. 'Miniature Pumped Fluid Loop Regulating Payload under Simulated Earth Albedo Heat Load on Radiator'. In: *47th International Conference on Environmental Systems*. Charleston, SC, USA, July 2017. URL: http://hdl.handle.net/2346/72917.

[2] Alex Lidow et al. '1.2 The Gallium Nitride Journey Begins'. In: *GaN Transistors for Efficient Power Conversion (3rd Edition)*. John Wiley & Sons, 2020. ISBN: 978-1-11959-4-147. URL: https://app.knovel.com/hotlink/khtml/id:kt0125DYR8/gan-transistors-efficient/gan-sic-compared-with.

[3] Alex Lidow et al. '17. Replacing Silicon Power MOSFETs'. In: *GaN Transistors for Efficient Power Conversion (3rd Edition)*. John Wiley & Sons, 2020. ISBN: 978-1-11959-4-147. URL: https://app.knovel.com/hotlink/khtml/id:kt0125E6C1/gan-transistors-efficient/new-capabilities-enabled.

[4] Alex Lidow et al. '3. Driving GaN Transistors'. In: *GaN Transistors for Efficient Power Conversion (3rd Edition)*. John Wiley & Sons, 2020. ISBN: 978-1-11959-4-147. URL: https://app.knovel.com/hotlink/khtml/id:kt0125DZL1/gan-transistors-efficient/driving-ga-introduction.

[5] Jim Williams. *High Voltage, Low Noise, DC/DC Converters*. Application note. Analog Devices, Mar. 2008. URL: https://www.analog.com/media/en/technical-documentation/application-notes/an118fb.pdf.

[6] Mojtaba Forouzesh et al. 'Step-Up DC–DC Converters: A Comprehensive Review of Voltage-Boosting Techniques, Topologies, and Applications'. In: *IEEE Transactions on Power Electronics* 32.12 (2017), pp. 9143–9178. DOI: 10.1109/TPEL.2017.2652318.

[7] Boris Axelrod, Yefim Berkovich and Adrian Ioinovici. 'Switched-Capacitor/Switched-Inductor Structures for Getting Transformerless Hybrid DC–DC PWM Converters'. In: *IEEE Transactions on Circuits and Systems I: Regular Papers* 55.2 (2008), pp. 687–696. DOI: 10.1109/TCSI.2008.916403.

[8] Sanghyeon Park, Jun Yang and Juan Rivas-Davila. 'A Hybrid Cockcroft–Walton/Dickson Multiplier for High Voltage Generation'. In: *IEEE Transactions on Power Electronics* 35.3 (2020), pp. 2714–2723. DOI: 10.1109/TPEL.2019.2929167.

[9] Gaetano Palumbo and Domenico Pappalardo. 'Charge Pump Circuits: An Overview on Design Strategies and Topologies'. In: *IEEE Circuits and Systems Magazine* 10.1 (2010), pp. 31–45. DOI: 10.1109/MCAS.2009.935695.

[10] I.C. Kobougias and E.C. Tatakis. 'Optimal design of a Half-Wave Cockroft-Walton Voltage Multiplier with minimum total capacitance'. In: *2008 IEEE Power Electronics Specialists Conference*. 2008, pp. 1104–1109. DOI: 10.1109/PESC.2008.4592077.

[11] J.S. Brugler. 'Theoretical performance of voltage multiplier circuits'. In: *IEEE Journal of Solid-State Circuits* 6.3 (1971), pp. 132–135. DOI: 10 . 1109/JSSC.1971.1049670.

[12] Naseer Ahmed, Noman Khan and Tanveer Abbas. 'An Inverter-Fed Cockcroft-Walton Multiplier Based High Voltage DC Source for Tokamak'. In: *2022 International Conference on Emerging Trends in Electrical, Control, and Telecommunication Engineering (ETECTE)*. 2022, pp. 1–6. DOI: 10.1109/ETECTE55893.2022.10007169.

[13] Christian Maennel. 'Improvement in the modelling of a half-wave Cockroft-Walton voltage multiplier'. In: *The Review of scientific instruments* 84 (June 2013), p. 064701. DOI: 10.1063/1.4807703.

[14] Mohsen Ruzbehani. 'A Comparative Study of Symmetrical Cockcroft-Walton Voltage Multipliers'. In: *Journal of Electrical and Computer Engineering* 2017 (Jan. 2017), pp. 1–10. DOI: 10.1155/2017/4805268.

[15] *Low IQ boost/SEPIC/Flyback/Inverting Converter with 0.5A, 140V Switch.* LT8331. Rev. C. Linear Technology. 2015. URL: https://www.analog.com/media/en/technical-documentation/data-sheets/LT8331.pdf.

[16] Lew Andrew R. Tria, Daming Zhang and John E. Fletcher. 'Planar PCB Transformer Model for Circuit Simulation'. In: *IEEE Transactions on Magnetics* 52.7 (2016), pp. 1–4. DOI: 10.1109/TMAG.2016.2516995.

[17] Sanghyeon Park, Lei Gu and Juan Rivas-Davila. 'A Compact 45 V-to-54 kV Modular DC-DC Converter'. In: *2019 20th Workshop on Control and Modeling for Power Electronics (COMPEL)*. 2019, pp. 1–7. DOI: 10.1109/COMPEL.2019.8769612.

[18] William Gerard Hurley et al. 'A Unified Approach to the Calculation of Self- and Mutual-Inductance for Coaxial Coils in Air'. In: *IEEE Transactions on Power Electronics* 30.11 (2015), pp. 6155–6162. DOI: 10.1109/TPEL.2015.2413493.

[19] M.M Góngora-Nieto et al. 'Impact of air bubbles in a dielectric liquid when subjected to high field strengths'. In: *Innovative Food Science & Emerging Technologies* 4.1 (2003), pp. 57–67. ISSN: 1466-8564. DOI: https://doi.org/10.1016/S1466-8564(02)00067-X. URL: https://www.sciencedirect.com/science/article/pii/S146685640200067X.

[20] 'IEEE Guide for Reliability-Based Placement of Overhead and Underground Switching and Overcurrent Protection Equipment up to and Including 38 kV'. In: *IEEE Std 1806-2021* (2021), pp. 1–52. DOI: 10 . 1109 / IEEESTD . 2021.9508912.

[21] Younsi Abdelkrim et al. 'Electrostatic Precipitator Having a Spark Current Limiting Resistors and Method for Limiting Sparking'. US 2011/0005388 A1. 13th Jan. 2011.

[22] Henry Ibekwe. 'Realization of a low-cost Op-Amp based PID Controller'. In: (June 2018). DOI: 10.13140/RG.2.2.29981.00485.

[23] TDK Electronics. 'Ferrites and accessories ER 9.5/5'. In: (2022). URL: https://www.sciencedirect.com/science/article/pii/S146685640200067X.

[24] Nor Azmi et al. '5 V to 6 kV DC-DC Converter Using Switching Regulator with Cockcroft-Walton Voltage Multiplier for High Voltage Power Supply Module'. In: *Recent Advances in Electrical & Electronic Engineering (Formerly Recent Patents on Electrical & Electronic Engineering)* 11 (June 2018). DOI: 10.2174/2352096511666180605094827.

[25] Sohiful Anuar Zainol Murad et al. 'A Novel 1.6 kV High Voltage Low Current Step-Up DC-DC Converter with Cockroft-Walton Voltage Multiplier for Power Supply Modules'. In: *Jurnal Teknologi* 81 (Aug. 2019). DOI: 10.11113/jt.v81.13411.

[26] Sanghyeon Park, Lei Gu and Juan Rivas-Davila. '60 V-to-35 kV input-parallel output-series DC-DC converter using multi-level class-DE rectifiers'. In: *2018 IEEE Applied Power Electronics Conference and Exposition (APEC)*. 2018, pp. 2235–2241. DOI: 10.1109/APEC.2018.8341327.

[27] Hyukjae Kwon et al. 'Analytical Modeling and Design of 27.12 MHz Single-Switch DC–DC Converter With PCB Transformer'. In: *IEEE Access* 11 (2023), pp. 12742–12754. DOI: 10.1109/ACCESS.2023.3242010.

[28] N. Dai et al. 'A comparative study of high-frequency, low-profile planar transformer technologies'. In: *Proceedings of 1994 IEEE Applied Power Electronics Conference and Exposition - ASPEC'94*. 1994, 226–232 vol.1. DOI: 10.1109/APEC.1994.316395.

[29] BSI Standards Publication. *Safety requirements for electrical equipment for measurement, control, and laboratory use – Part 1: General requirements.* BS EN 61010-1:2010. London, UK: BSI, 2010.

A   Appendix

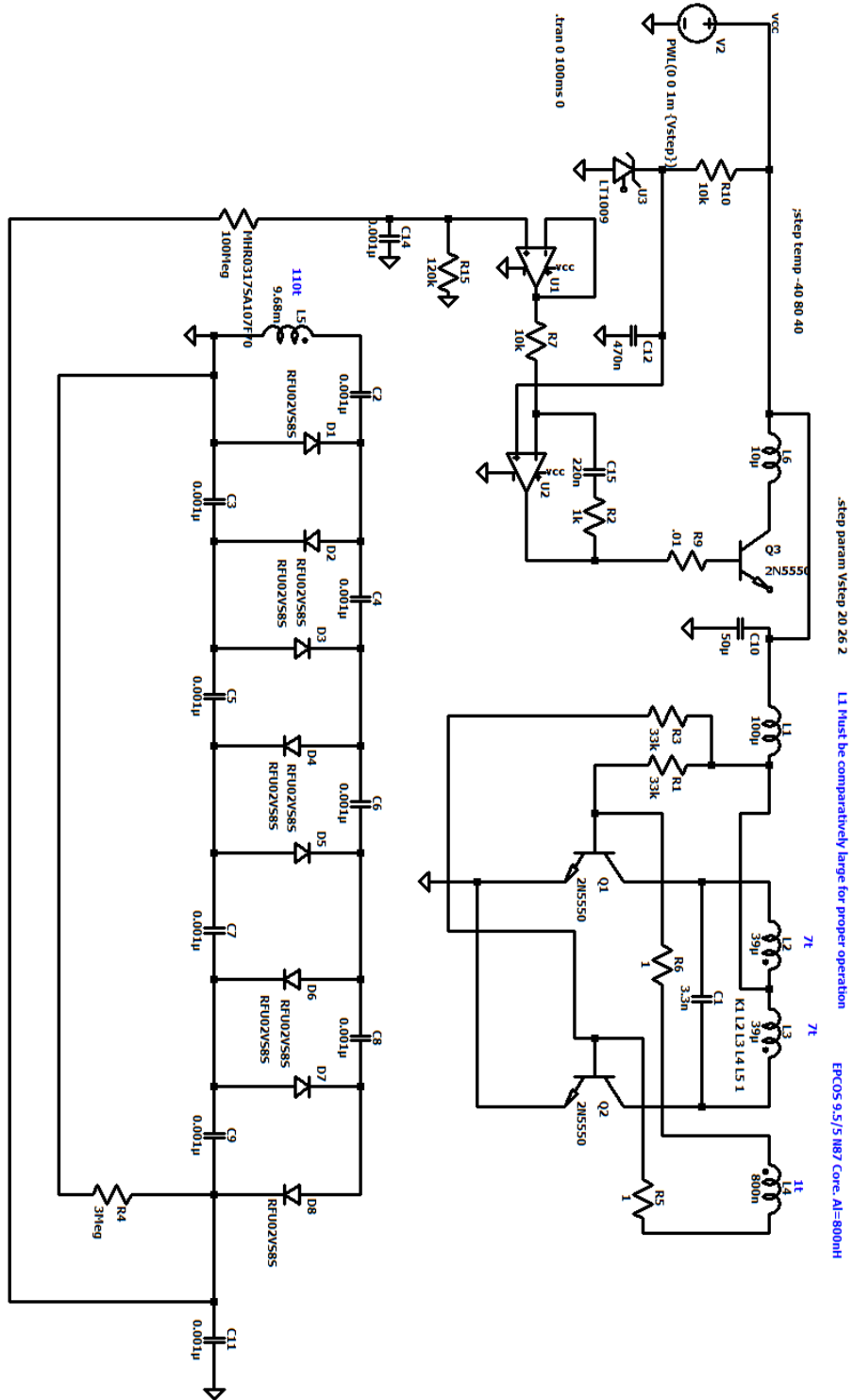## A.1   Conventional Royer-based converter

Figure 22: Conventional Royer-based converter LT-spice schematic

Table 8: List of components used in the conventional royer based converter. The sum of all costs in the table is 7.03 €. The prices are based on the unit price when purchasing 1000 units from Mouser. Other components includes low voltage resistors and capacitors. The price of the transformer is based on a old offer given to APR.

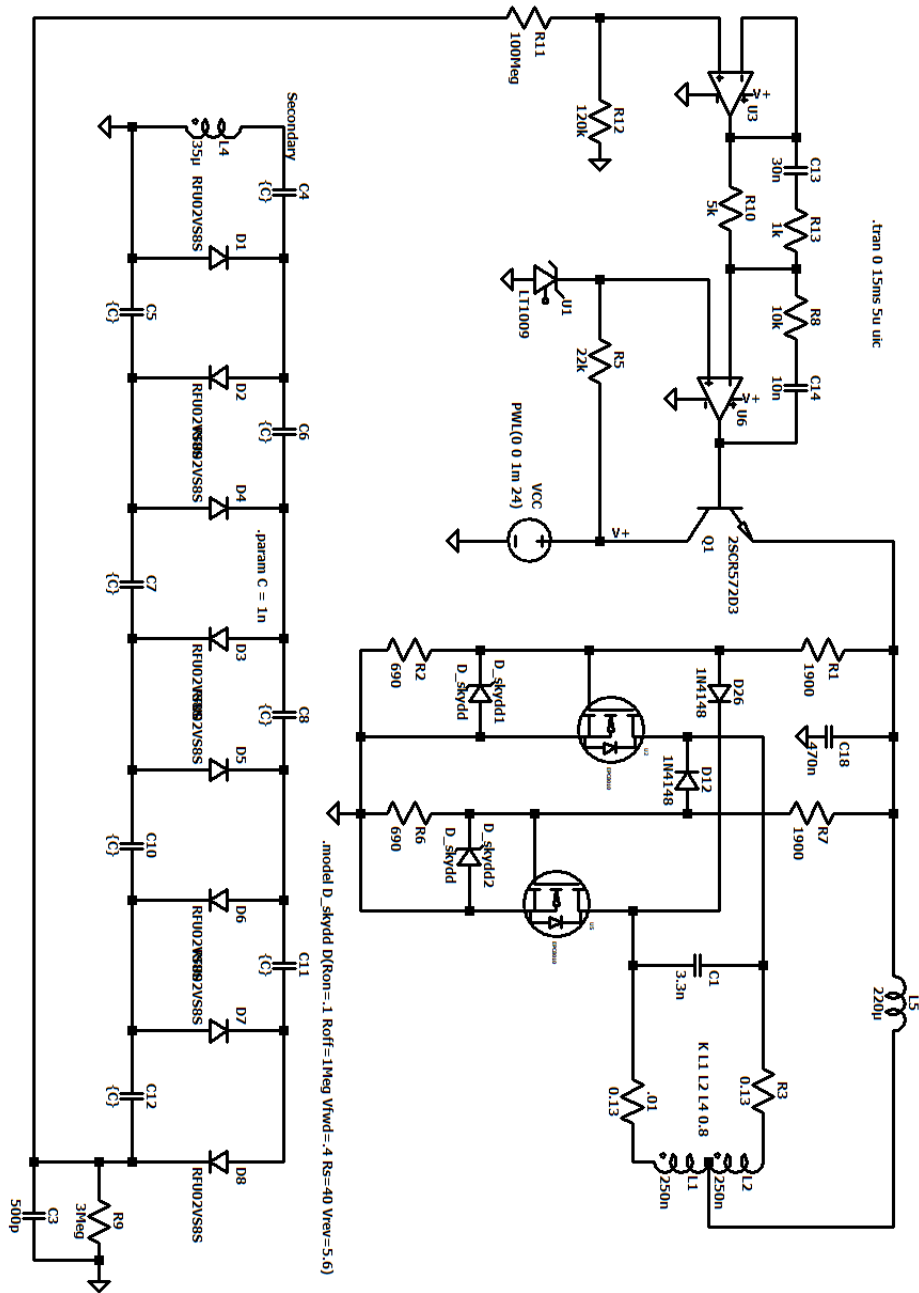| Component	Number or units	Unit price
NPN 2n5550	3	0.09 €
Resistor 51Meg 2kv CHV2010-JW-516ELF	2	0.14 €
OP DUAL NCV20072DR2G	1	1.15 €
Diode 600v RFU02VSM6STR	9	0.09 €
1nF Wurth 885342208011	8	0.09 €
BandGapRef LT1009CD	1	0.88 €
100uH B82462A4104K000	1	0.66 €
Transformer	1	1.34 €
Other components	-	1 €

A.2 High-frequency Royer-based converter

Figure 23: High frequency Royer based converter with air-core planar transformer LTspice schematic.

Table 9: List of components used in the High frequency based converter with a planar air-core transformer. The sum of all costs in the table is 7.02 €. The prices are based on the unit price when purchasing 1000 units from Mouser. An exception was made for EPC8010 which was purchased from Digikey since it was not available at Mouser. Other components includes low voltage resistors and capacitors.

| Component	Number or units	Unit price
GaNMOS EPC8010	2	0.98 €
NPN 2SCR572D3TL1	1	0.38 €
OP DUAL NCV20072DR2G	1	1.15 €
BandGapRef LT1009CD	1	0.88 €
Resistor 51Meg 2kv CHV2010-JW-516ELF	2	0.14 €
Diode 600v RFU02VSM6STR	9	0.09 €
1nF Wurth 885342208011	8	0.09 €
BandGapRef LT1009CD	1	0.88 €
220uH SDR0603-221KL	1	0.24 €
Protection Diode BZX84C5V6LT3G	2	0.03 €
Other components	-	0.5 €

A.3 Transformerless converter
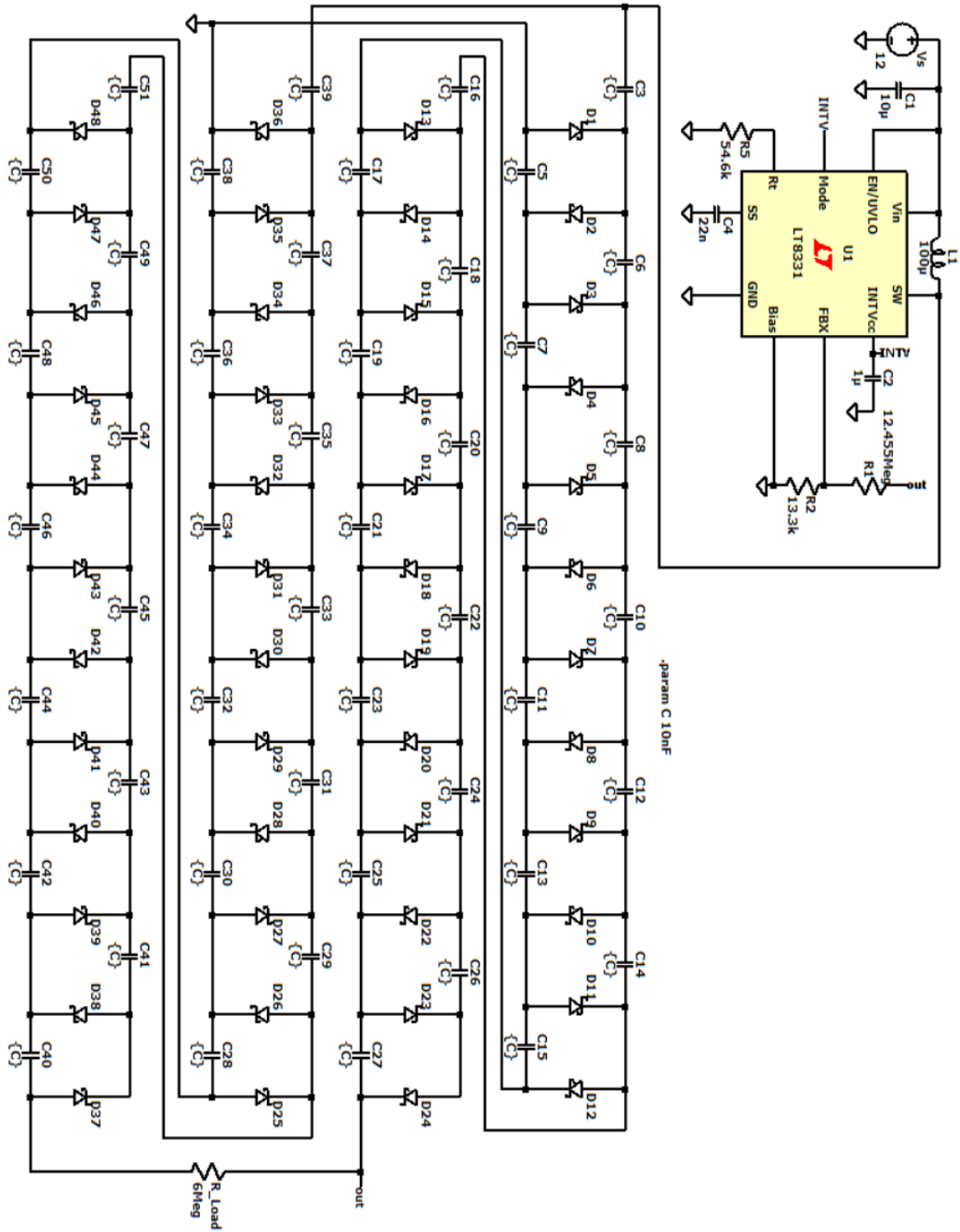
Figure 24: Transformerless converter LTspice schematic.

Table 10: List of components used in the transformerless converter. The sum of all costs in the table is 10.36 €. The prices are based on the unit price when purchasing 1000 units from Mouser.

Component	Number or units	Unit price
Inductor (100uH) SRU1048-101Y	1	0.44 €
Diode BAV21WS-7-F	43	0.04 €
Capacitor (10uF) GRM21BR61H106KE43L	1	0.08 €
Capacitor (1uF) CL21B105KAFNNNG	1	0.02 €
Capacitor (0.22uF) CL21B224KBFNFNE	1	0.02 €
Capacitor (8200pF) C0805C822KBRACTU	43	0.06 €
Boost Converter LT8331 LT8331EMSE#PBF	1	4.98 €
Resistor (160k) RK73H2ATTD1603F	1	0.01 €
Resistor (100Meg) CRHA1206AF100MFKEF	1	0.74 €
Resistor (56.2k) CR0805-FX-5622ELF	1	0.01 €